surements is a strong confirmation of the theory. The solid line in the figure shows that $H_B R_C$ is nearly proportional to $1 - T/T_c$. We obtain a similar temperature dependence by using expressions for $H_B R_C$ involving other measured properties of superfluid B-He^3.

In conclusion, we have shown that the orientation of B-He^3 in a parallel plate geometry is consistent with the theoretical analysis of the surface anisotropy in I. We have also found that a careful analysis of the effects of bending in our geometry is consistent with the earlier analysis of NMR results in cylindrical geometries.

The authors wish to thank P. W. Anderson, E. I. Blount, and C. M. Varma for helpful conversations.

*On sabbatical leave from the University of Massachusetts, Amherst, Mass. Work supported in part by National Science Foundation Grant No. NSF DMR 74-18030.

†Work performed while at Bell Laboratories.

[1]P. Balian and N. R. Werthamer, Phys. Rev. 131, 1553 (1963).

[2]D. D. Osheroff, Phys. Rev. Lett. 33, 1009 (1974).

[3]R. A. Webb, R. L. Kleinberg, and J. C. Wheatley, Phys. Rev. Lett. 33, 145 (1974).

[4]L. R. Corruccini and D. D. Osheroff, to be published. See also Ref. 2.

[5]T. J. Greytak, R. T. Johnson, S. N. Paulson, and J. C. Wheatley, Phys. Rev. Lett. 31, 452 (1973).

[6]A. I. Ahonen, M. T. Kaikala, M. Krusius, and O. V. Lounasmaa, Phys. Rev. Lett. 33, 628 (1974).

[7]D. D. Osheroff and P. W. Anderson, Phys. Rev. Lett. 33, 686 (1974).

[8]W. F. Brinkman, H. Smith, D. D. Osheroff, and E. I. Blount, Phys. Rev. Lett. 33, 624 (1974).

[9]D. D. Osheroff and W. F. Brinkman, Phys. Rev. Lett. 32, 584 (1974).

[10]A. J. Leggett, Ann. Phys. (New York) 85, 11 (1974).

[11]C. M. Varma and N. R. Werthamer, Phys. Rev. A 9, 1465 (1974).

[12]This effect is a generalization to arbitrary values of α of Leggett's prediction (Ref. 10) of a small shift in g value for B-He^3.

[13]S. Engelsberg, W. F. Brinkman, and P. W. Anderson, Phys. Rev. A 9, 2592 (1974).

Two-Dimensional Stability of an Electromagnetic Wave Obliquely Incident on a Nonuniform Plasma*

D. W. Forslund, J. M. Kindel, Kenneth Lee, and E. L. Lindman
University of California, Los Alamos Scientific Laboratory, Los Alamos, New Mexico 87544
(Received 29 October 1974)

For an electromagnetic wave obliquely incident on an inhomogeneous plasma, the dominant instability at critical density is a radiating decay instability whose associated ion-wave frequency, even in regimes where the growth rate greatly exceeds the real frequency, is approximately $(\lambda_D^2 L)^{-1/3} c_s \equiv k_{\min} c_s$. The stimulated radiation peaks between the normal and backscatter angles and may be an important factor in explaining present experiments. A nonlinear calculation at modest power shows that the nonlinear state involves a large-amplitude ion wave through which the excited waves can compress the pump wave.

An electromagnetic wave incident on a plasma at an angle to the density gradient can be absorbed resonantly by linear mode conversion into the electron plasma wave if the incident wave is polarized in the plane of incidence.[1] The stability of the resulting field structure is of considerable interest in laser-target experiments[2] and microwave-heating experiments.[3] In fact, recently the stability of such a structure has been examined in a laboratory plasma.[3] Thus far the only theoretical treatment of the problem has been within the WKB approximation and the electrostatic limit.[4] Here we present a rather general analysis where the pump wave is self-consistently calculated and the excited waves are treated by the full electromagnetic wave equations.

The field structure which forms after linear mode conversion in a hot plasma is known and has been described elsewhere.[2] These are the equations about which we want to make linear perturbations.

For a hot-fluid plasma we combine the electron momentum and continuity equations with Maxwell's equations, assuming an adiabatic pressure law for the electrons and neglecting the ion motion on the high-frequency waves. We take electric fields and wave vectors of the incident and unstable waves polarized in the x-y plane (plane

of incidence) and consider a plasma density gradient along x. The incident (pump) electromagnetic wave of frequency ω_0 is assumed to impinge on the plasma profile at an angle $\theta \equiv \sin^{-1}(k_{y0}/k)$ with an electric field in vacuum varying as $[\hat{x}E_{x0}(x,t) + \hat{y}E_{y0}(x,t)]\exp(ik_{y0}y - i\omega_0 t)$.

The waves considered to be excited by the pump are two high-frequency waves whose electric fields vary as $E_\pm(x,t)\exp[i(k_y \pm k_{y0})y \pm i\omega_0 t]$ and a low-frequency ion wave whose density varies as $n_L(x,t)\exp(ik_y y)$. For the ion wave we assume quasineutrality, although we have solved the set of equations described below without this assumption with similar results.

The equations describing the high-frequency electric fields of the linearly excited waves are given by

$$c^2[\nabla^2\vec{E}^\pm - \nabla(\nabla\cdot\vec{E}^\pm)] \mp 2i\omega_0\frac{\partial\vec{E}^\pm}{\partial t} + [\omega_0^2 - \tilde{\omega}_{pe}^2]\vec{E}^\pm + \tilde{v}_e^2\left[3\nabla(\nabla\cdot\vec{E}^\pm) - \nabla\cdot\vec{E}^\pm\,\frac{\nabla n_0(x)}{n_0}\right] = \frac{n_L}{2n_0}\omega_{pe}^2\hat{O}(\vec{E}_0), \tag{1}$$

where $\nabla \to \hat{x}\partial/\partial x + \hat{y}ik_y^\pm$, $\tilde{\omega}_{pe}^2 \equiv \omega_{pe}^2/(1 + i\nu_\pm/\omega_0)$, $\tilde{v}_e^2 = v_e^2/(1 + i\nu_{L\pm}/\omega_0)$, and where $\hat{O}(\vec{E}_0) = \vec{E}_0$ for the plus wave and $\hat{O}(\vec{E}_0) = \vec{E}_0^*$ for the minus wave. The damping $\nu_\pm$ is the usual collisional damping on the light and plasma waves; $\nu_{L\pm}$ is an effective Landau damping which is put in the pressure term to preferentially damp the electrostatic part of the high-frequency waves (see Forslund *et al.*, Ref. 1). $v_e = (T_e/m_e)^{1/2}$ is the electron thermal velocity, $n_0(x)$ is the zero-order density, and $k_y^\pm = k_y \pm k_{y0}$. By standard arguments the ion-wave equation is the usual ion-acoustic-wave equation with a $\nabla(E^2)$ driving term:

$$\frac{\partial^2 n_L}{\partial t^2} + 2\gamma_d\frac{\partial n_L}{\partial t} - c_s^2\left[\nabla^2 n_L - \nabla\cdot\left(n_L\frac{\nabla n_0}{n_0}\right)\right] = \frac{e}{2M_i\omega_0 c}\nabla\cdot(n_0\nabla F), \tag{2}$$

where

$$F \equiv \vec{E}_0\cdot\vec{E}^- + \vec{E}_0^*\cdot\vec{E}^+, \qquad \nabla \to \hat{x}\partial/\partial x + \hat{y}ik_y.$$

The equations for the pump wave are identical in form to Eq. (1) for the plus wave except that (A) the right-hand side is zero and $\partial/\partial t \to 0$ if we do not include feedback on the pump, or (B) the right-hand side is replaced by $\frac{1}{2}\omega_{pe}^2(E^{-*}n_L/n_0 + E^+ n_L^*/n_0)$ and $\partial/\partial t \neq 0$ if we include feedback to the pump. Additionally, there should be a dependence of $n_0(x)$ on E_0 which arises because of the secular change in the profile due to the zero-order ponderomotive force. For simplicity it has been neglected here. This general problem of profile modification in light-wave absorption has been treated elsewhere.[5] Because of the important results of a steepening of the density profile at the critical surface ($\omega_0 = \omega_{pe}$), we consider only relatively steep density profiles.

If we Fourier analyze the ion wave in time, i.e., let $\partial/\partial t \to -i\omega$, then the plus and minus waves described by Eq. (1) have frequencies $\omega \pm \omega_0$. The linear system then consists of five coupled second-order complex differential equations in x. We numerically solve[6] these equations iteratively determining the complex ω which gives rise to absolute instability, i.e., $\mathrm{Im}(\omega) > 0$.

For relatively sharp gradients, $k_0 L \lesssim 25$, we have determined that the most unstable mode is one in which near threshold the minus wave (which is larger than the plus wave) is very similar in structure to the pump wave. The ion wave has a slightly shorter "wavelength" $k \sim k_{\min} \equiv (\lambda_D^2 L)^{-1/3}$ with a frequency $\omega \approx k_{\min} c_s$. It is tempting to identify the instability as a decay type. In Fig. 1 we plot a typical solution for the magnitudes of the pump and excited waves as a function of position x. Figures 1(a) and 1(d) are the x and y components of the pump electric field; Figs. 1(b) and 1(e) are the x and y components of the electric field of the minus wave. Figure 1(c) is the magnitude of E_x^+ as a function of x. The absolute values of the excited waves are, of course, arbitrary in this eigenvalue problem; however, Fig.

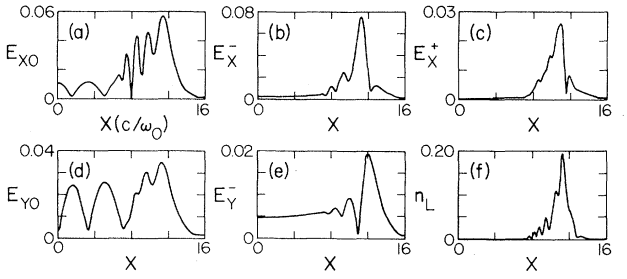

FIG. 1. The magnitude of the x electric field of (a) the pump wave, (b) the minus wave, and (c) the plus wave versus position in units of c/ω_0; (d) the magnitude of the pump E_y versus x; (e) the magnitude of E_y^- versus x; (f) the magnitude of n_L in units of the critical density versus position. Electric fields are in units $eE/m_e\omega_0 c$. Parameters are $v_0/c = 0.015$, $T_e/m_e c^2 = 0.005$, $k_0 L = 10$, $M_i/m_e = 100$, $T_e/T_i \gg 1$, $\sin\theta = 0.4$, and $k_y c/\omega_0 = 0$. The density profile is a linear density ramp with the critical density at $x = 12.25c/\omega_0$ and $v_0 \equiv eE_0/m_e\omega_0$.

1(c) illustrates the point that the plus wave has a smaller relative amplitude because it is somewhat off resonance. In Fig. 1(f) we plot the magnitude of the low-frequency ion wave (normalized to the critical density) as a function of x. For this case $\omega/\omega_0 \approx 0.018 + (0.011)$.

Note that the excited waves have a peak amplitude at the Airy-function maximum of the pump wave. The "wavelength" of the excited minus wave is slightly shorter than that of the pump wave which has a wavelength around the critical density of $\lambda \approx 2\pi(\lambda_D^2 L)^{1/3}$. As one nears threshold the "wavelength" or width of the excited minus wave becomes nearly identical to that of the pump. At higher powers this width of the most unstable wave becomes even shorter as also does the width of the ion wave which satisfies approximate k matching. The large electromagnetic component to the excited waves is seen in Fig. 1(e) by comparing the E field at the left boundary to the electrostatic maximum which occurs just below critical density (which is at $x = 12.25c/\omega_0$). At backscatter angles, i.e., $k_y c/\omega_0 \approx 0.8$, this electromagnetic component is even larger. In two-dimensional plasma simulations we have seen the eigenfunctions which have been calculated here over the k_y range which we expect to be unstable.

An important issue is that of threshold.[4,7] Simple heuristic arguments from infinite homogeneous plasma theory, where growth rates balance the damping ν_{eff} due to convective loss of the plasma wave [where $\nu_{\text{eff}} \approx \omega_0(\lambda_D/L)^{2/3}$], yield the correct scaling on temperature and density gradients. Noting that the maximum $E_x \propto (k_0 L)^{-1/2} \times (L/\lambda_D)^{2/3} E_0$, we find the threshold is given by $v_0/v_e > 5(k_0 L)^{1/2}\lambda_D/L$. The numerical factor was determined by an exact calculation of Eqs. (1) and (2), assumed zero damping on the ion wave, and assumed damping much less than ν_{eff} on the excited high-frequency waves.

In Fig. 2(a) we plot the real frequency (dashed curve) and the growth rate (solid curve) of the excited waves as a function of v_0/c for the same parameters as in Fig. 1. At high powers, i.e., $\gamma \gg \nu_{\text{eff}}$, the growth rate appears to scale as E_0 while near threshold it scales as E_0^2. Additionally, both the real frequency and growth rate appear to scale as $(m_e/M_i)^{1/2}$. It is interesting that for increasing power the real frequency drops slightly although $\gamma \gg \text{Re}(\omega)$. In Fig. 2(b), for the parameters of Fig. 1 except $v_0/c = 0.05$, we plot the growth rate (solid) and real frequency (dashed) as a function of k_y for the ion wave. The growth rate for $k_0 L = 2.5$ is also given for comparison.

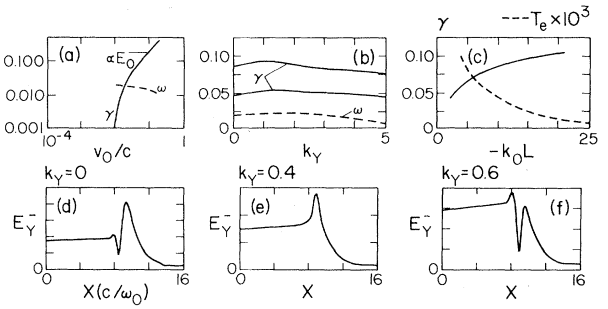

FIG. 2. All parameters in (a)–(f) are the same as in Fig. 1 unless otherwise specified. (a) Frequency (dashed curve) and growth rate (solid curve) versus $v_0 = eE_0/m_e\omega_0$. (b) Frequency (dashed curve) and growth rate (solid curve) versus k_y of the ion wave for $v_0/c = 0.05$. The lower solid curve is the growth rate for $k_0 L = 2.5$. (c) Growth rate versus T_e/mc^2 and $k_0 L$ for $v_0/c = 0.05$. For $k_0 L = 2.5$, $\sin\theta = 0.4$, and $v_0/c = 0.03$, the magnitude of E_y for the minus wave for (d) $k_y = 0$, (e) $k_y = 0.4$, and (f) $k_y = 0.6$. The absolute value of E_y is arbitrary and the critical density is at $x = 9.25c/\omega_0$.

Note that both maximize near the backscatter angle, $k_y c/\omega_0 \approx 0.8$, but drop for increasing k_y. This is a behavior one might expect from an oscillating two-stream instability with finite frequency due to finite-k driver, although the scaling of $\text{Re}(\omega)$ with ion mass may not be expected. Figure 2(c) is a plot of growth rate versus $k_0 L$ and T_e/mc^2; $\sin\theta$ is changed to keep the absorption at 40%; $v_0/c = 0.05$ and other parameters not varying are the same as in Fig. 1. For some regime where $\gamma \gg \nu_{\text{eff}}$, it appears that $\gamma \propto E_0 L^{1/3}/T_e$ approximately, although a simple power law seems inappropriate.

In Figs. 2(d)–2(f), we plot the magnitude of E_y as a function of x for $k_y = 0$, 0.4, and 0.6, respectively; $v_0/c = 0.03$, $k_0 L = 2.5$, and $\sin\theta = 0.4$. The important point to observe is the large radiation out of the plasma, which peaks between an angle normal to the target ($ck_y/\omega_0 = 0.4$) and the backscatter angle ($ck_y/\omega_0 = 0.8$). For the parameter range considered, this coupling to the electromagnetic field does not significantly affect the growth rates and threshold conditions which are basically electrostatic in origin, but does provide an important external diagnostic. In two-dimensional plasma simulations we have seen such stimulated scattering which was first observed by Biskamp and co-workers. We believe that the stimulated backscatter observed in experiments may really be this decay instability of the resonant absorption pump wave. Note that the threshold in terms of external power is extremely low

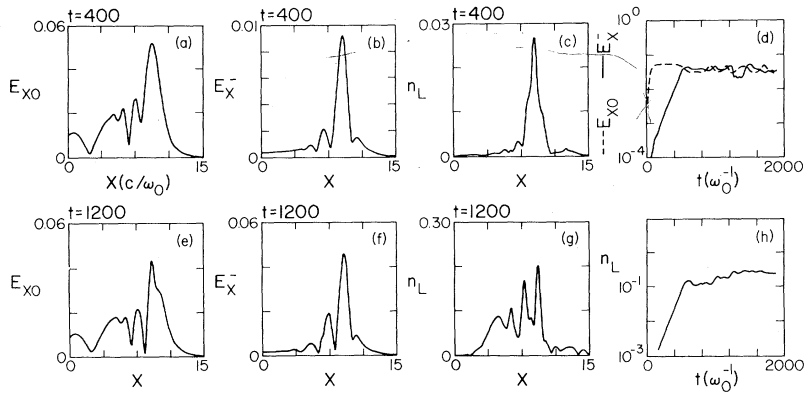

FIG. 3. The linear and nonlinear behavior of the instability with the parameters of Fig. 1 except that $k_y = 0.8$. At the time $t = 400\omega_0^{-1}$ in the linear regime the amplitudes versus position are E_x of (a) the pump wave, (b) the minus wave, and (c) n_L of the ion wave. (d) The time history of the maximum E_x of the pump wave (dashed) and the minus wave (solid). At $t = 1200\omega_0^{-1}$ in the nonlinear regime the amplitudes versus position are E_x of (e) the pump wave, (f) the minus wave, and (g) n_L of the ion wave. (h) The time history of the maximum n_L of the ion wave.

in terms of present laser-target experiments.

We have also numerically solved Eqs. (1) and (2) and the corresponding equation for the pump wave in time and space by means of Laasonen differencing[6] and the usual Gaussian elimination procedure. The pump wave is turned on slowly, reaches equilibrium, and then causes the plus and minus waves to grow from noise with an associated growth of the low-frequency ion wave. In the linear regime the growth rates, real frequency, and the eigenfunctions agree very well with the stability calculation given above. For parameters the same as in Fig. 1 but with $k_y = 0.8$, the structure of the E_x field of the pump wave, the minus wave, and the density perturbation of the ion wave are shown in the linear regime at the time $400\omega_0^{-1}$ in Figs. 3(a)–3(c). The only noise used was an initially smooth ion density perturbation.

The importance of three different saturation mechanisms have been considered. These are pump depletion, nonlinear damping on the plasma wave, and nonlinear damping on the ion wave. Near threshold, pump depletion seems to dominate. Somewhat above threshold the low-frequency density perturbation becomes as large as the background and ion trapping should be important. Only very strong plasma-wave damping, $\nu_L/\omega_0 \gg n_1/n_0$ (where n_1 is the density perturbation of the plasma wave), is able to stabilize the instability far above threshold. Mode coupling between many closely spaced k_y modes may also be an important stabilization mechanism not considered here.

In Fig. 3(d) we show the time history of the maximum E_x field of the pump wave and the minus wave for the problem cited above. Note the exchange of energy between the pump and the excited wave after the initial saturation due to pump depletion. From Fig. 3(h) we see that the maximum low-frequency ion-wave density saturates at ~0.1 to 0.3, small enough that ion trapping is not significant. At higher power the saturated value of n_L is larger. As the pump is depleted, its shape is also distorted as shown in Fig. 3(e). At this point it takes on the shape of the excited wave shown in Fig. 3(f) which has a slightly shorter wavelength. One can view this as a local trapping of the pump which is even more pronounced at higher powers. The energy emitted by the minus wave saturates at about 5–10% of the incident pump energy. The total energy absorption after saturation becomes an oscillatory function with an amplitude of ~10% of the incident energy flux. From Fig. 3(g) we see that the ion wave develops secondary maxima which propagate down the density gradient.

*Work performed under the auspices of the U. S. Atomic Energy Commission.

[1]R. B. White and F. F. Chen, Plasma Phys. 16, 565 (1974); D. W. Forslund, J. M. Kindel, K. Lee, E. L. Lindman, and R. L. Morse, LASL Report No. LA-UR-74-894 (to be published), and references therein.

[2]P. Lee, D. V. Giovanelli, R. P. Godwin, and G. H. McCall, Appl. Phys. Lett. 24, 406 (1974); K. Eidman and R. Sigel, Max-Planck-Institut für Plasmaphysik,

Garching, Report No. IPP IV/46, 1972 (unpublished); B. H. Ripin, J. M. McMahon, E. A. McLean, W. M. Manheimer, and J. A. Stamper, Phys. Rev. Lett. 33, 634 (1974); L. M. Goldman, J. Soures, and M. J. Lubin, Phys. Rev. Lett. 31, 1184 (1973). This is only a partial list.

[3]H. C. Kim, R. L. Stenzel, and A. Y. Wong, Phys. Rev. Lett. 33, 896 (1974); R. L. Stenzel, A. Y. Wong, and H. C. Kim, Phys. Rev. Lett. 32, 654 (1974).

[4]R. B. White, C. S. Liu, and M. N. Rosenbluth, Phys. Rev. Lett. 31, 520 (1973).

[5]D. W. Forslund, J. M. Kindel, K. Lee, and E. L. Lindman, LASL Report No. LA-5542-PR, 1973 (unpublished), p. 67; E. J. Valeo and W. L. Kruer, Phys. Rev. Lett. 33, 750 (1974); D. W. Forslund, J. Kindel, K. Lee, and E. L. Lindman, LASL Report No. LA-UR-74-1636 (unpublished).

[6]R. D. Richtmyer and K. W. Morton, *Difference Methods for Initial Value Problems* (Interscience, New York, 1967), p. 199 ff and p. 189.

[7]F. W. Perkins and J. Flick, Phys. Fluids 14, 2012 (1971); M. N. Rosenbluth, Phys. Rev. Lett. 29, 565 (1972); D. F. Dubois, D. W. Forslund, and E. A. Williams, Phys. Rev. Lett. 33, 1013 (1974).

Space Correlation in Ion-Beam–Plasma Turbulence

D. Grésillon, F. Doveil, and J. M. Buzzi
Laboratoire de Physique des Milieux Ionisés, Ecole Polytechnique, 91120 Palaiseau, France*
(Received 9 September 1974)

We investigate the turbulence excited by an ion beam in an unmagnetized plasma in connection with the linear theory of the ion-beam–plasma instability. Depending on beam velocity, one- or three-dimensional turbulence can be expected. These two types are experimentally observed by looking at space correlation functions.

The turbulence generated by beam-plasma interaction is known to diffuse particles in velocity space. Among the processes by which such diffusion occurs, theory[1] has pointed to the effect of unstable electrostatic waves propagating off angle from the beam velocity. Thus, whereas the E field can only be axial in one-dimensional (1D) systems, it can be oblique in 3D plasmas. The particle velocities are not only decelerated or accelerated, but also deviated.[2] This 3D effect has an important bearing on the final state of the interaction.[3] The object of this paper is to present a correlation method for measuring the structure of this random E-field turbulence. We chose the ion-beam–plasma system since its most unstable modes are off axis, unlike with the electron beam. Moreover, the occurrence of oblique propagation in this type of turbulence was seen in numerical results,[4] and observed in an experiment in which discrete frequency components[5] were correlated.

We first establish the 3D predictions of the linear theory of the ion-beam instability.[6] Experimental results obtained by correlation techniques are reported, showing two types of turbulence: plane 1D turbulence and 3D turbulence with oblique E fields.

The 3D linear instability.—The 3D dispersion relation for electrostatic waves in an unmagnetized plasma is written[7]

$$1+\sum_s \frac{\omega_s^2}{n_s k^2}\int d^3v(\omega-\vec{k}\cdot\vec{v})^{-1}\vec{k}\cdot\frac{\partial f_s}{\partial \vec{v}}=0, \qquad (1)$$

where the sum is over species s (electrons, plasma ions, and beam ions) of distribution function f_s and plasma frequency $\omega_s=(n_s e^2/\epsilon_0 m_s)^{1/2}$.

The distributions are assumed Maxwellian. A 1D solution[6] to Eq. (1) depends on four parameters: beam velocity V_b, relative density, relative temperature, and plasma-ion–to–electron temperature ratio. The 3D analysis introduces two new parameters: the perpendicular temperatures of the beam and of the plasma ions. Fortunately, the double-plasma-machine[8] method of ion-beam formation provides a useful simplification. The ions of the source plasma are assumed to have the same density and temperature as the plasma ions. Accelerating the source ions between two plane grids changes their parallel distribution into a positive tail of a truncated Maxwellian,[6,9] with uniquely defined density, velocity, and temperature, while the perpendicular temperature is unchanged. The electron–to–plasma-ion temperature ratio and the beam velocity are the only parameters left. Once these are known, Eq. (1) can be solved for each orientation (and modulus) of $\vec{k}$ to give the frequency and growth rate of unstable modes.